Journal of Hydrology 603 (2021) 126881

Contents lists available at ScienceDirect

Journal of Hydrology

journal homepage: www.elsevier.com/locate/jhydrol

A novel integrated method based on a machine learning model for estimating evapotranspiration in dryland

Tonglin Fu [a,b,c], Xinrong Li [a,*], Rongliang Jia [a], Li Feng [a]

[a] Shapotou Desert Research and Experiment Station, Northwest Institute of Eco-Environment and Resources, Chinese Academy of Sciences, Lanzhou, China
[b] University of Chinese Academy of Sciences, Beijing, China
[c] School of Mathematics and Statistics, Longdong University, Qingyang, China

ARTICLE INFO

This manuscript was handled by Andras Bardossy, Editor-in-Chief, with the assistance of Sheng Yue, Associate Editor

Keywords:
Evapotranspiration
Variational mode decomposition
Grey wolf optimizer algorithm
Support vector machine
Tengger Desert

ABSTRACT

Evapotranspiration (ET) plays a vital role in the water cycle and energy cycle and serves as an important linkage between ecological and hydrological processes. Accurate estimation of ET based on data-driven methods is of great theoretical and practical significance for exploring soil evaporation, plant transpiration and the regional hydrological balance. Most existing estimation approaches were proposed based on multiple meteorological variables. This study proposed a novel hybrid estimation approach to estimate the monthly ET using only historical ET time series in the southeastern margins of the Tengger Desert, China. The approach consisted of three sections including data preprocessing, parameter optimization and estimation. The model evaluation demonstrated that the hybrid model based on the variational mode decomposition (VMD) method, grey wolf optimizer (GWO) algorithm and support vector machine (SVM) model achieved superior computational performance compared to the performance of other methods. The Nash–Sutcliffe coefficient of efficiency (NSCE) increased from 0.8588 to 0.8754 and the mean absolute percentage error (MAPE) decreased from 28.42% to 23.22% in the testing stage. Thus, we suggest that the hybrid VMD-GWO-SVM model will be the best choice for estimating ET in the absence of regional meteorological monitoring.

1. Introduction

Evapotranspiration (ET) is the sum of the vegetation transpiration and soil evaporation capacity within a certain period, which is closely related to meteorological parameters (precipitation, solar radiation, wind speed and temperature), soil moisture, vegetation traits and other factors (Eagleson, 2002; Rodríguez-Iturbe and Porporato, 2004; Feng et al., 2016; Wu et al., 2020). ET plays a vital role in the water cycle and energy cycle and is also an important linkage between ecological and hydrological processes (Li et al., 2016; Fan et al., 2018). Therefore, how to precisely estimate ET is a core issue for understanding the water cycle regime in soil–plant-atmosphere continuous systems (Li et al., 2016; Malik et al., 2018).

Traditional ET estimation methods are mainly physically based methods (Wu et al., 2020; Liu et al., 2020), such as the Priestley–Taylor (Priestley and Taylor, 1972), Hargreaves (Hargreaves and Samani, 1985), corrected FAO-24 Penman (Allen and Pruitt, 1991), and FAO-56 Penman-Monteith (Feng et al., 2016) methods, which have great limitations in accurately estimating ET in cases lacking meteorological parameters (e.g., solar radiation, wind speed, and air temperature) (Feng et al., 2016; Fan et al., 2018; Wu et al., 2020). However, machine learning models are likely to solve similar issues due to not requiring any assumptions (Rezaie-Balf et al., 2017; Wang et al., 2017; Wu et al., 2020). Current machine learning models include multilayer perceptron (Traore et al., 2016), long short-term memory (Majhi et al., 2019), radial basis function neural networks (Petković et al., 2016), multilayer artificial neural networks (Keskin and Terzi, 2006; Jain et al., 2008; Wu et al., 2020), extreme learning machine (Abdullah et al., 2015; Feng et al., 2016; Gocic et al., 2016; Wu et al., 2020; Zhu et al., 2020), genetic programming (Shiri et al., 2012), self-organizing map neural networks (Malik et al., 2018), support vector machine (SVM) (Wen et al., 2015), and random forest (Feng et al., 2017). As the structure and parameters of machine learning models also affect computing accuracy (Gocić et al., 2015; Wang et al., 2019; Wu et al., 2020), machine learning models hybridized with swarm intelligence algorithms (e.g., the whale optimization algorithm, genetic algorithm, particle swarm optimization algorithm, firefly algorithm, and quantum-performed particle swarm optimization algorithm) are often used to overcome these shortcomings,

* Corresponding author.
E-mail address: lxinrong@lzb.ac.cn (X. Li).

https://doi.org/10.1016/j.jhydrol.2021.126881
Received 26 June 2021; Accepted 22 August 2021
Available online 8 September 2021

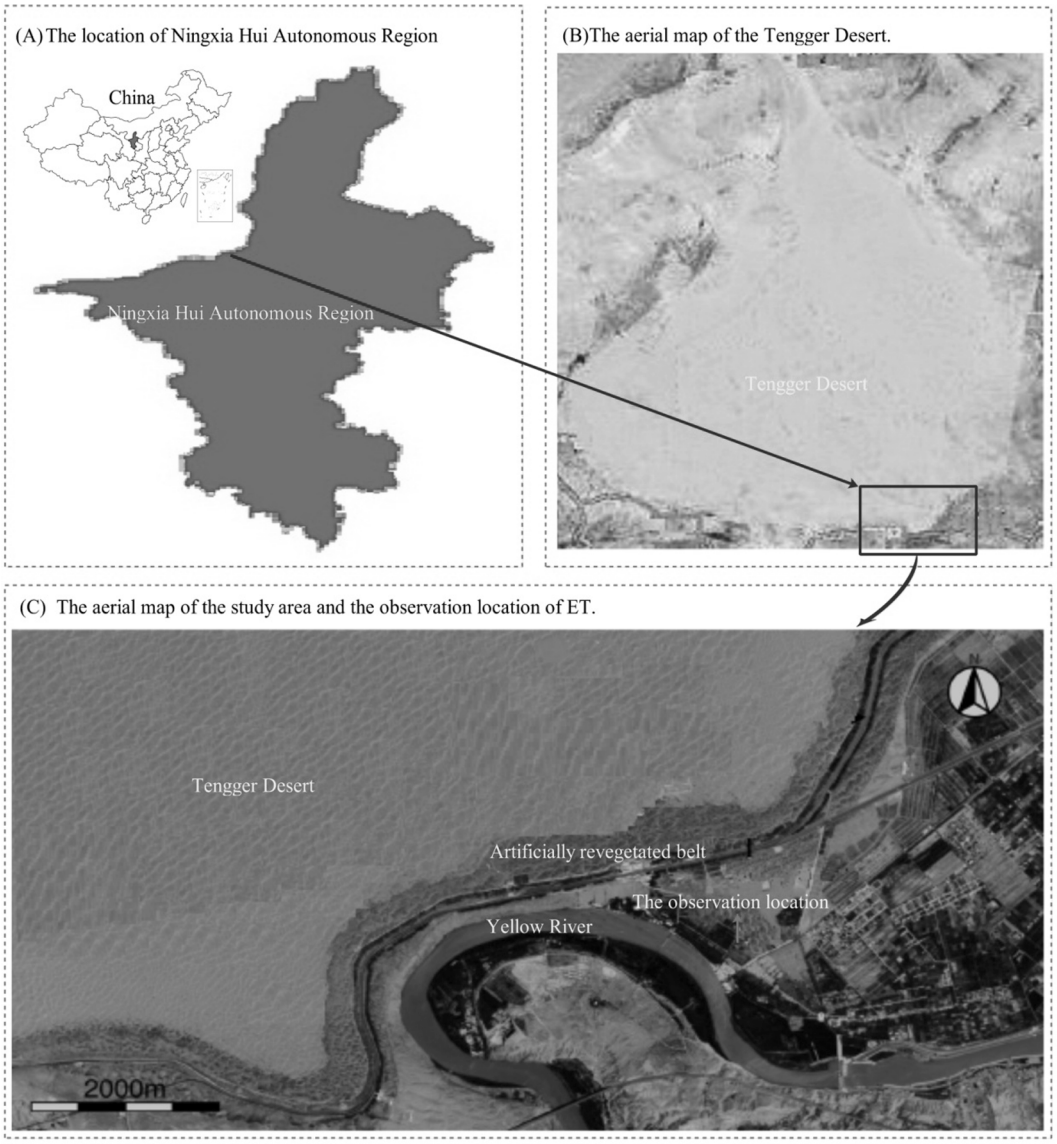

Fig. 1. The geographical of the study area. (A) The location of Ningxia Hui Autonomous Region. (B) The aerial map of the Tengger Desert. (C) The aerial map of study area and the observation location of ET.

allowing them to be the best choice for estimating ET (Gocić et al., 2015; Petković et al., 2016; Yin et al., 2017; Moazenzadeh et al., 2018; Wu et al., 2020; Zhu et al., 2020).

ET is largely dependent on precipitation, air temperature, wind speed, barometric pressure, airflow, and humidity; and these parameters are usually influenced by the local landform and geomorphological traits (Li et al., 2016; Feng et al., 2016; Moazenzadeh et al., 2018; Wu et al., 2020). Furthermore, ET is also determined by the soil moisture and vegetation traits (Eagleson, 2002; Rodríguez-Iturbe and Porporato, 2004; Li et al., 2018). As above, the factors affecting ET are complex, and the collected ET time series are highly nonlinear and exhibit seasonal irregularity (Pammar and Deka, 2017). Given this situation, only using a machine learning model may not be able to handle nonlinear data when preprocessing of the collected data is not performed (Gocić et al., 2015; Pammar and Deka, 2017; Rezaie-Balf et al., 2019). In this context, machine learning models coupled with the discrete wavelet transform (DWT) (Gocić et al., 2015; Pammar and Deka, 2017) or ensemble empirical mode decomposition (EEMD) (Rezaie-Balf et al., 2019) to estimate ET using only historical ET time series were proposed (Gocić et al., 2015; Pammar and Deka, 2017; Rezaie-Balf et al., 2019). Nevertheless, wavelet technology has the disadvantage of sensitivity to the selection of thresholds, and EEMD suffers from an intrinsic drawback of endpoint effects (Dragomiretskiy and Zosso, 2014; Zuo et al., 2020). Variational mode decomposition (VMD) is a more robust and self-adaptive data preprocessing method than DWT and EEMD, and thus VMD is widely used to extract effective features from nonlinear and nonstationary time series Dragomiretskiy and Zosso, 2014; Zuo et al.,2020); however, few studies use VMD to extract the main variation features from the observed ET time series for more precise estimation.

Due to the highly nonlinear physical process and intrinsic complexity of ET, combining multiple methods to establish a hybrid estimation model without adequate meteorological data remains highly desirable (Feng et al., 2016; Wu et al., 2020; Zhu et al., 2020). In this paper, we proposed a series of hybrid models based on data preprocessing techniques, including the DWT, EEMD and VMD, the grey wolf optimizer (GWO) algorithm (Mirjalili et al., 2014), and the SVM, to estimate ET using the existing observed ET from January 1991 to December 2018 in the southeastern margins of the Tengger Desert, China. First, the DWT, EEMD, and VMD were employed to extract the basic characteristics from nonstationary ET time series separately in order to counterbalance the weakness of directly estimating ET, which may lead to large errors. The best data preprocessing technique was chosen according to the signal-to-

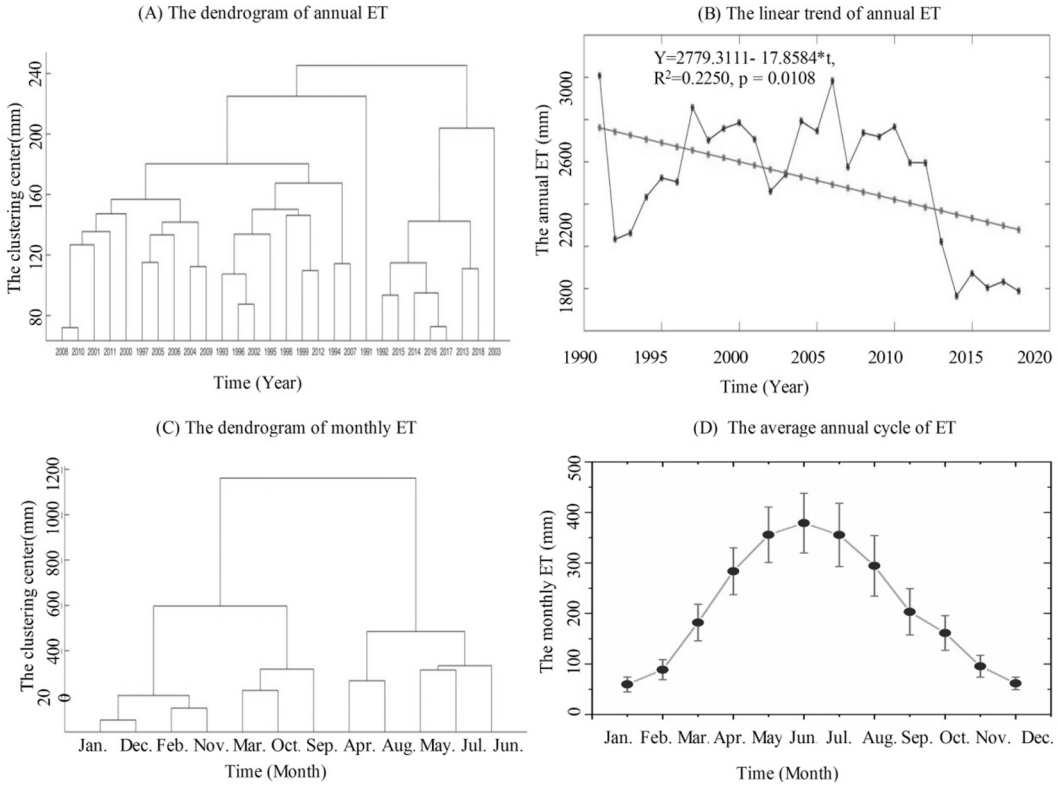

Fig. 2. The statistical descriptions of collected ET data at different time scales from 1991 to 2018. (A) The dendrogram of k-means clustering for annual ET. (B) The linear trend of annual ET from 1991 to 2018. (C) The dendrogram of monthly ET. (D) The average annual cycle of ET.

noise ratio (SNR) and root mean squared error (RMSE). Second, the GWO algorithm was employed to optimize the penalty coefficient and radius of the kernel function of the SVM to overcome the sensitivity of parameter selection. Third, the hybrid VMD-GWO-SVM, EEMD-GWO-SVM, DWT-GWO-SVM, VMD-SVM, EEMD-SVM, DWT-SVM, and GWO-SVM models and single SVM model were used to estimate the monthly ET. Finally, the computing performances of the proposed models were compared using the evaluation criteria of the Nash–Sutcliffe coefficient of efficiency (NSCE), Pearson's correlation coefficient (PCC), the mean absolute percentage error (MAPE), the normalized mean squared error (NMSE), the mean absolute error (MAE) and the RMSE. The most suitable estimation model was selected from the proposed models based on the comparison results. Compared to previous studies (Gocić et al., 2015; Pammar and Deka, 2017; Moazenzadeh et al., 2018; Rezaie-Balf et al., 2019; Wu et al., 2020), the aims of this study are to establish a novel hybrid estimation model based on VMD, GWO and the SVM. This proposed model is able to simultaneously account for parameter optimization and data preprocessing, achieve better computing performance than the other proposed hybrid and single SVM models, and can be applied to estimate ET without adequate meteorological parameters.

2. Materials and methods

2.1. 1. Study area and data collection

The study site is located in the Shapotou region of the southeastern margins of the Tengger Desert (37°32′ N, 105°02′ E), Ningxia Hui Autonomous Region, China. The average annual precipitation was 180.57 mm, and the annual evaporation was 2520.4 mm. Soil evaporation is the main way of water loss while precipitation is the main source of soil water recharge in the southeastern margins of the Tengger Desert, where the underground water level exceeds 60 m deep. The location of the study area is illustrated in Fig. 1.

The monthly ET data were collected from the meteorological monitoring data from 1991 to 2018 by Shapotou Desert Research and Experiment Station, Chinese Academy of Sciences. Statistical descriptions of collected ET data at different time scales from 1991 to 2018 are shown in Fig. 2. Using K-means clustering, the ETs in 1992, 2003, and from 2013 to 2018 were grouped into one category; and the other ETs were grouped into another category (Fig. 2A). Furthermore, the annual ET time series had a significantly decreasing trend and highly nonlinear characteristics (Fig. 2B), and the ET from April to August differed from that during other months (Fig. 2C). April - August is just in the growing season (from April to September) (Fig. 2D). In addition, the principles of K-means clustering and linear trend analysis are mentioned in the Appendix.

2.2. Theoretical model and calculation method

In this study, data preprocessing techniques, including the DWT, EEMD and VMD, were used to eliminate chaotic noise and extract effective features for collected ET data (the principles of the DWT, EEMD, and VMD are mentioned in the Appendix; and the flowcharts of the DWT, EEMD and VMD are shown in Fig. 3A). In the data preprocessing, the single ET time series was decomposed into multiple additive signals, and a few signals were chosen from these. To obtain the best data preprocessing performance, the SNR and RMSE were chosen as the criteria to determine the optimal parameters of each data preprocessing technique and evaluate the denoising performance of the DWT, EEMD and VMD (Rezaie-Balf et al., 2019; Zuo et al., 2020).

The DWT was used with Daubechies wavelet order 4 (db4) because db4 has only three wavelet filter coefficients with exact reconstruction possibilities (Gocić et al., 2015; Pammar and Deka, 2017). To obtain the decomposed wavelet coefficients, db4 with levels 1 to 7 was tested, and the SNR and RMSE were selected as the benchmarks to determine the optimal decomposition level. As for EEMD, the number of intrinsic mode

The flowchart of proposed monthly evapotranspiration estimating models

Step 1.The observed ET time series were decomposed by using the DWT,EEMD and VMD, respectively.

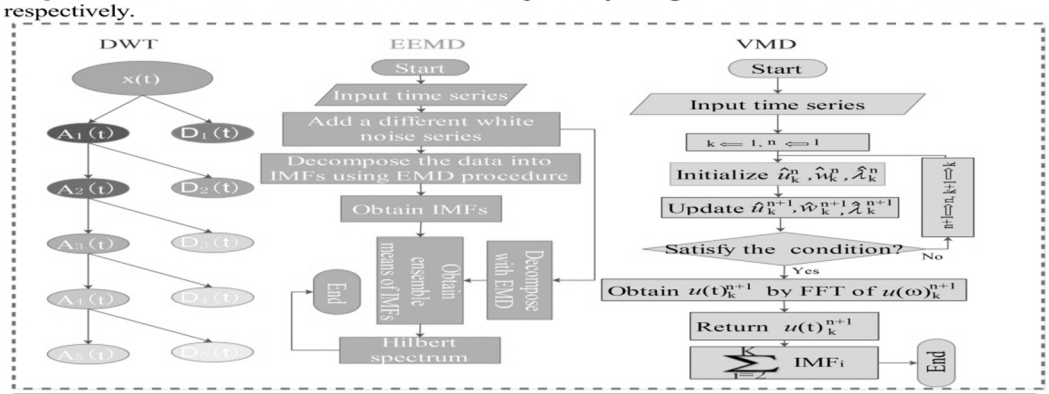

(A) The flowcharts the of DWT, EEMD and VMD

Step 2.The denoising performance of the DWT,EEMD and VMD were compared based on the SNR and RMSE.

Step 3.The longitudinal data selection method was employed to determine the input-output structure of the SVM.

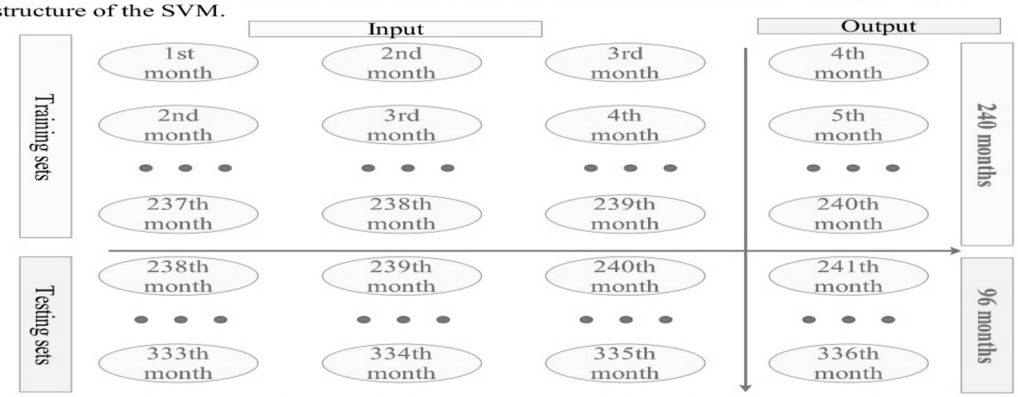

(B) The schematic of the longitudinal data selection method

Step 4. The GWO algorithm was employed to optimize the hyperparameters of the SVM.

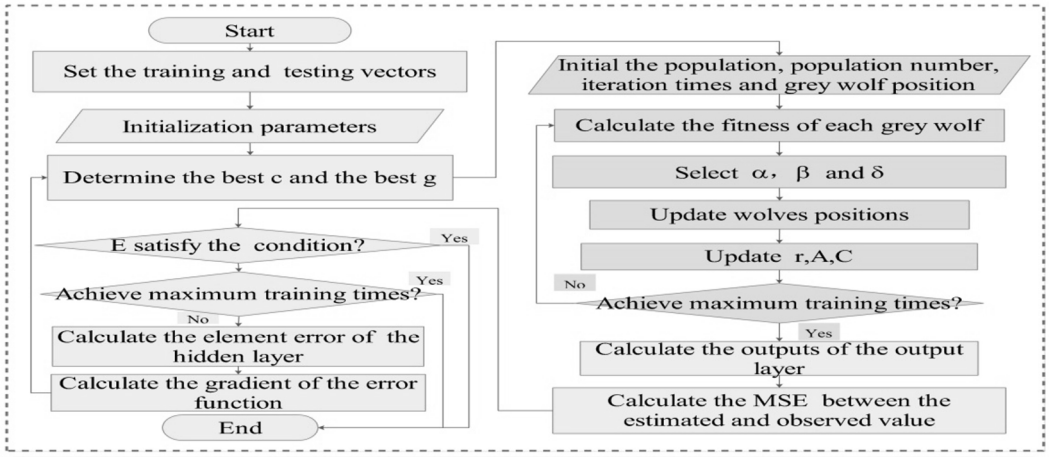

(C) The flowchart of GWO-SVM

Step 5. The hybrid models and single SVM model were used to estimate the monthly ET.

Step 6. The computing performance were compared according to the evaluation indexes.

Fig. 3. The flowchart of the proposed models. (A) The flowchart of DWT, EEMD and VMD. (B) The schematic of the longitudinal data selection method. (C) The flowchart of GWO-SVM.

functions (IMFs) was 8, which was determined by $[log_2(n)]$, where $[\cdot]$was the least integer function and $n$was the length of the input data (Wu and Huang, 2009). The final standard deviation of error ε_{ne} was controlled with $\varepsilon_{ne} = \varepsilon/\sqrt{NE}$, where the number of ensemble members$NE = 500$ and the amplitudes of the added white noise$\varepsilon = 0.1, 0.15, 0.2, 0.25, 0.3, 0.35$, and 0.4, respectively. The optimal amplitude of the added white noise and the outputs of EEMD were determined according to the maximum SNR and the minimum RMSE. The parameters of VMD are$\alpha = 0.05$ and$\tau = 0$, where α is the balancing parameter of the data fidelity constraint and τ is the time step of the dual ascent (Dragomiretskiy and

Table 1
Evaluation metrics.

Metric	Definition	Equation
NSCE	Nash-Sutcliffe coefficient of efficiency	$NSCE = 1 - \sum_{i=1}^{n}\left(x_i - \widehat{x}_i\right)^2 / \sum_{i=1}^{n}(x_i - \overline{x})^2$
PCC	Pearson's correlation coefficient	$PCC = \frac{\sum_{i=1}^{n}(x_i - \overline{x})(\widehat{x}_i - \overline{x})}{\sqrt{\sum_{i=1}^{n}(x_i - \overline{x})^2}\sqrt{\sum_{i=1}^{n}(\widehat{x}_i - \overline{x})^2}}$
MAPE	Mean absolute percentage error	$MAPE = \frac{1}{n}\sum_{i=1}^{n}\left\|\frac{x_i - \widehat{x}_i}{x_i}\right\| \times 100\%$
NMSE	Normalized mean squared error	$NMSE = \frac{1}{n}\sum_{i=1}^{n}\left(\frac{x_i - \widehat{x}_i}{x_i}\right)^2$
RMSE	Root mean squared error	$RMSE = \sqrt{\frac{1}{n}\sum_{i=1}^{n}\left(x_i - \widehat{x}_i\right)^2}$
MAE	Mean absolute error	$MAE = \frac{1}{n}\sum_{i=1}^{n}\left\|x_i - \widehat{x}_i\right\|$
SNR	Signal noise ratio	$SNR = 10log_{10}\left(\sum_{i=1}^{n}x_i^2 / \sum_{i=1}^{n}\left(x_i - \widehat{x}_i\right)^2\right)$

Note: x_i denotes the observed data and $\widehat{x}_i$ denotes the estimated data.

Zosso, 2014). The maximum number of modes $K_{max}$was obtained if the SNR and RMSE stopped changing (Zuo et al., 2020), the reasonable pre-estimation of K was $K_{max}-1$, and the KthIMF was discarded as chaotic noise. The new time series generated by the DWT, EEMD and VMD were fed to the machine learning model to estimate the ET.

The SVM is a widely used machine learning model that can efficiently adapt to the nonlinear characteristics of ET change compared to statistical models and artificial neural networks (Feng et al., 2016; Mehdizadeh et al., 2017; Fan et al., 2018). The main description of the SVM is provided in the Appendix, and the longitudinal data selection method was adopted to determine the data structure of the integrated method (Zhao et al., 2019; Fu et al., 2020; Dong et al., 2021). A schematic of the longitudinal data selection method with input dimension $d = 3$ is shown in Fig. 3B. The optimal input dimension of each proposed model was determined by trial and error. The dataset from January 1991 to December 2010 (which had a total of 240 records or 72% of the entire dataset) was used as the training set, and the dataset from January 2011 to December 2018 (which had a total of 96 records or 28% of the entire dataset) was used as the testing set. The ratio between the training and testing sets was approximately 7:2. The output dimensions of all the proposed estimation models were 1, namely, 1 month ahead estimation was performed. The output vector consisting of the 241st through 336th elements of each proposed model was regarded as the estimation result (Fig. 3B). Before training the network, the input and output data were normalized using the min–max normalization method, which is defined as

$$x_i^{'} = \frac{x_i - x_{imin}}{x_{imax} - x_{imin}}, i = 1, 2, \cdots, n,$$

where $x_i^{'}$,x_i,x_{imin}, and x_{imax} are the normalized value, observed value, minimum value, and maximum value, respectively.

It is well known that the SVM is characterized by employing the kernel trick to convert the lower-dimensional input data to a higher-dimensional feature space implicitly and perform a linear regression in this feature space (Vapnik, 1998; Pammar and Deka, 2017; Rezaie-Balf et al., 2019). In the simulation processes, the radial basis function (RBF) was chosen as the kernel function of the SVM (Pammar and Deka, 2017), and the GWO algorithm was adopted to optimize the penalty - coefficient and the radius of the kernel function. Descriptions of the GWO algorithm are provided in the Appendix, and the flowchart of the GWO-SVM is shown in Fig. 3C. The SVM hybridized with the GWO algorithm is denoted as GWO-SVM, and VMD combined with the GWO-SVM is denoted as the VMD-GWO-SVM. The construction processes of the other hybrid EEMD-GWO-SVM, DWT-GWO-SVM, VMD-SVM, EEMD-SVM, DWT-SVM and GWO-SVM models are similar to that of the VMD-GWO-SVM. The MATLAB software (R2019a, Math Works, USA) was utilized to conduct all computing processes.

The flowchart of the proposed models is shown in Fig. 3, and the main steps of the proposed models are as follows:

Step 1. Data preprocessing techniques, including the DWT, EEMD and VMD, were used to decompose the monthly ET time series.

Step 2. The SNR and RMSE were used to determine the optimal parameters of the DWT, EEMD and VMD; and the best data preprocessing technique was chosen according to the SNR and RMSE.

Step 3. The collected ET time series and the outputs of the DWT, EEMD and VMD were divided into a training set and a testing set, respectively. The longitudinal data selection method was used to determine the input dimensions of the SVM.

Step 4. The GWO algorithm was used to optimize the hyper-parameters of the SVM.

Step 5. Hybrid VMD-GWO-SVM, EEMD-GWO-SVM, DWT-GWO-SVM, VMD-SVM, EEMD-SVM, DWT-SVM, and GWO-SVM models and a single SVM model were employed to estimate the monthly ET.

Step 6. The results of the proposed models were compared based on

Table 2
The denoising performance of the DWT, EEMD and VMD.

Method	Parameter	SNR	RMSE	Method	Parameter	SNR	RMSE	Method	Parameter	SNR	RMSE
DWT	db4 level1	40.8201	2.2127	EEMD	$\varepsilon = 0.1$	26.3839	11.6609	VMD	K = 3	28.846	8.7827
	db4 level2	38.7179	2.8186		$\varepsilon = 0.15$	22.7863	17.6445		K = 4	40.3406	2.3383
	db4 level3	37.8902	3.1004		$\varepsilon = 0.2$	24.2796	14.8575		K = 5	42.6451	1.7934
	db4 level4	37.5044	3.2412		$\varepsilon = 0.25$	23.6078	16.0522		K = 6	42.6616	1.79
	db4 level5	37.2924	3.3213		$\varepsilon = 0.3$	24.2422	14.9217		K = 7	42.6616	1.79
	db4 level6	37.1721	3.3676		$\varepsilon = 0.35$	24.2386	14.9277		K = 8	42.6616	1.79
	db4 level7	37.1362	3.3815		$\varepsilon = 0.4$	24.8232	13.9562		K = 9	42.6616	1.79

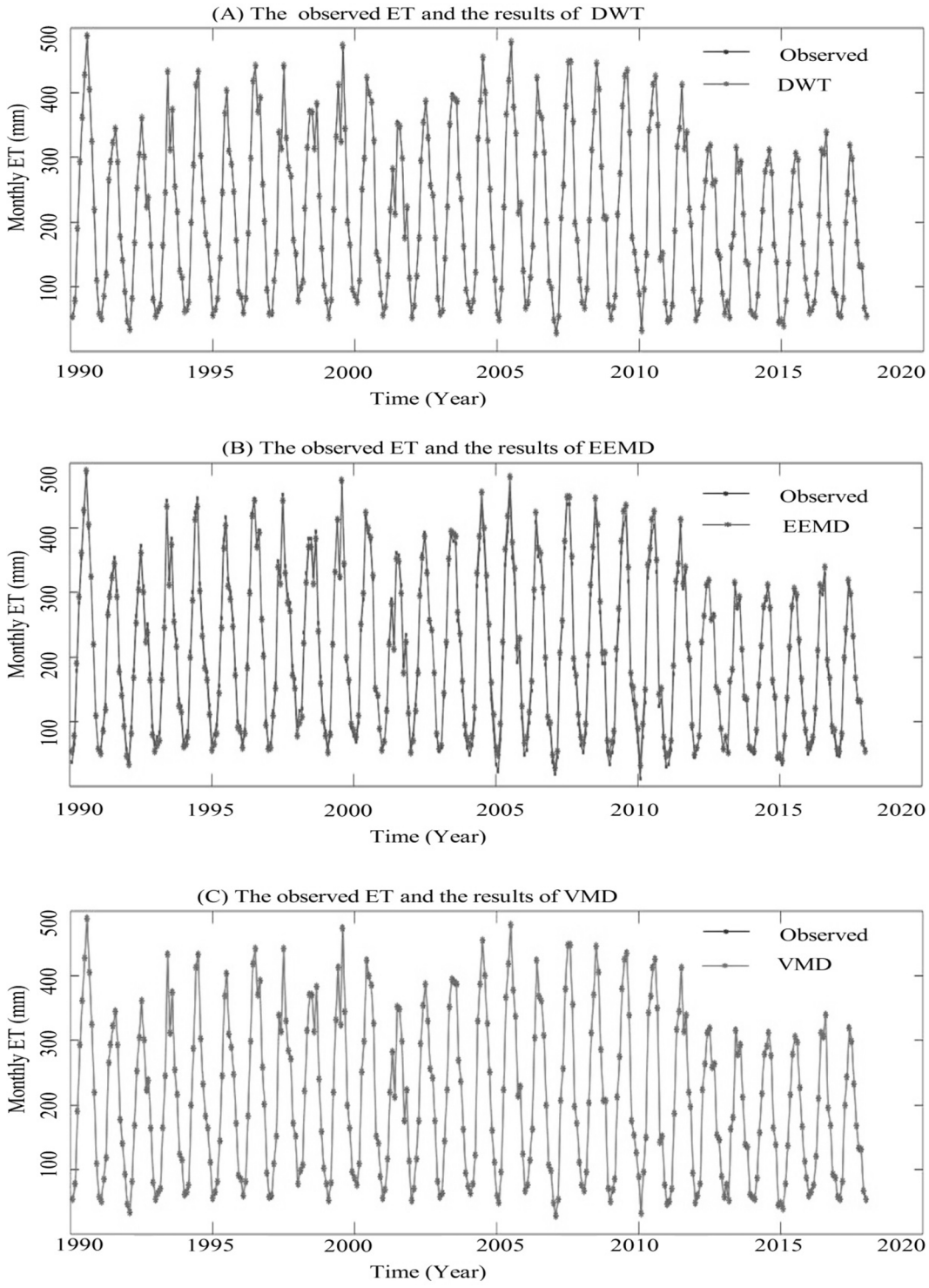

Fig. 4. The data preprocesses results of DWT, EEMD, and VMD. (A) The observed ET and the results of DWT. (B) The observed ET and the results of DWT. (C) The observed ET and the results of VMD.

the evaluation criteria of the NSCE, PCC, MAPE, NMSE, RMSE and MAE. The best hybrid model was chosen using the evaluation results.

2.3. Model performance assessment

The accuracy of the proposed models was evaluated with multiple evaluation indexes (Majhi et al., 2019; Wu et al., 2020; Dong et al., 2021); and the evaluation indexes of the SNR, NSCE, PCC, MAPE, NMSE, RMSE and MAE are defined in Table 1. Due to the different emphases of the evaluation index, the evaluation directions of different evaluation indexes may be inconsistent. E.g., the NSCE and PCC are dimensionless metrics with the same evaluation direction, implying that the higher the computing accuracy is, the closer the evaluation index is to 1. Furthermore, the MAPE, NMSE, RMSE, and MAE have the same evaluation direction, implying that the smaller their values are, the higher the computing accuracy of the proposed model. Therefore, the NSCE and PCC can be regarded as positive indicators; and the MAPE, NMSE, RMSE, and MAE can be regarded as negative indicators. If the results of

Table 3
The parameters set for each proposed model found during training that was then used for testing.

	Parameters	SVM	DWT-SVM	EEMD-SVM	VMD-SVM	GWO-SVM	DWT-GWO-SVM	EEMD-GWO-SVM	VMD-GWO-SVM
d =	C	1	1	1	1	55.8789	100	100	4.557
2	G	0.5	0.5	0.5	0.5	1.8911	1.2844	5.4948	8.2213
	MAPE	35.29%	34.99%	35.38%	34.93%	32.42%	31.80%	30.59%	31.23%
d =	C	1	1	1	1	100	16.0417	14.7823	86.0928
3	G	0.3333	0.3333	0.3333	0.3333	0.6406	1.5487	0.2564	0.7648
	MAPE	28.42%	27.94%	28.65%	27.46%	24.73%	25.22%	26.47%	23.21%
d =	C	1	1	1	1	55.4135	68.9681	94.2325	72.5743
4	G	0.25	0.25	0.25	0.25	0.7248	1.2431	0.7314	0.6521
	MAPE	31.65%	31.73%	31.32%	31.31%	24.14%	23.69%	26.23%	23.35%
d =	C	1	1	1	1	11.9326	89.3303	22.1642	11.617
5	G	0.2	0.2	0.2	0.2	0.9692	0.01162	0.01	1.2953
	MAPE	33.25%	32.66%	34.15%	33.15%	31.58%	31.89%	35.59%	32.06%
d =	C	1	1	1	1	43.7784	5.0003	31.7629	52.0301
6	G	0.1667	0.1667	0.1667	0.1667	0.42639	1.7186	2.5942	0.3707
	MAPE	35.39%	34.74%	36.43%	35.26%	30.46%	34.07%	34.00%	31.02%

Note: C denotes the penalty coefficient and G denotes the radius of the kernel function, where $G = 0.5\sigma^{-2}$.

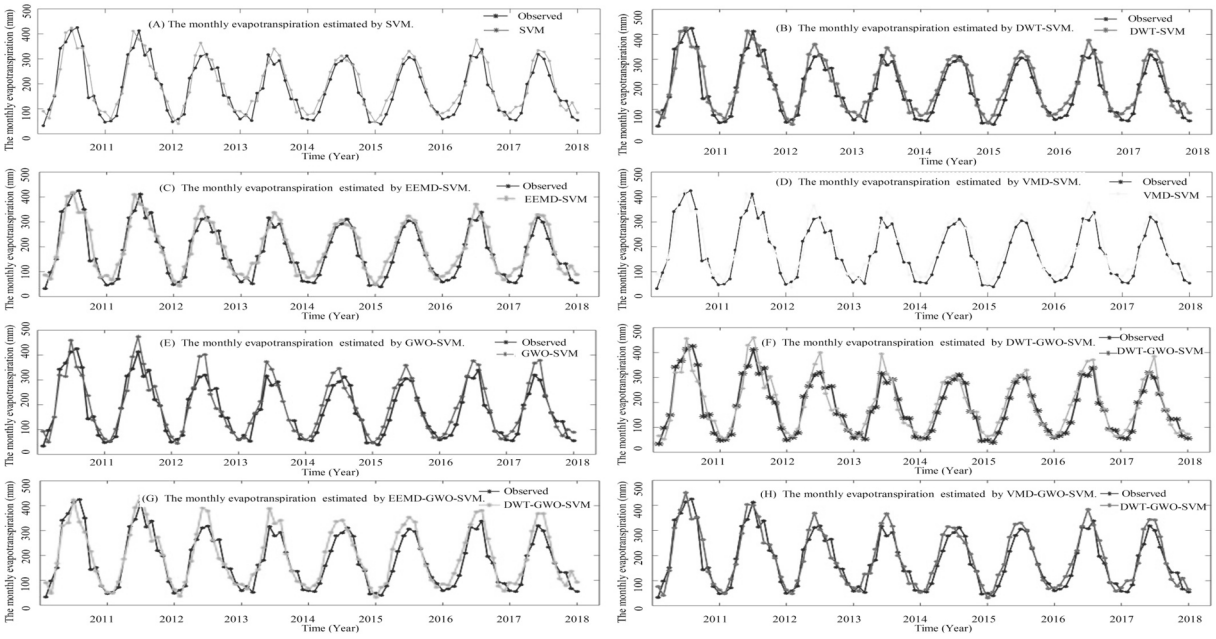

Fig. 5. The estimating results of proposed model. (A) The estimating result of SVM; (B)-(H) The estimating results of hybrid models.

the different evaluation indexes with the same evaluation direction are found to be inconsistent with each other, the NSCE and MAPE will be selected as the final benchmarks.

3. Results and discussion

3.1. Data preprocessing performance evaluation

Table 2 shows that the maximum SNR and minimum RMSE of the DWT were 40.8201 and 2.2127, respectively, suggesting that the best level of db4 was 1. As for EEMD, Table 2 indicates that the maximum SNR and minimum RMSE were 26. 3839 and 11.6609, suggesting that the best amplitude of the added white noise is $\varepsilon = 0.1$. In VMD, the reasonable pre-estimation of the number of modes is 5 since the SNR and RMSE remain unchanged for $K \geqslant 6$. The observed and generated ET time series of the DWT, EEMD and VMD with the optimal parameters are illustrated in Fig. 4.

Table 2 and Fig. 4 show that the DWT displayed better denoising performance than EEMD from the overall or local point of view. Nevertheless, this did not mean that the denoising performance of EEMD was generally inferior to that of the DWT. This occurred because the values at the starting and end points of the monthly ET time series were not necessarily extreme values, and the upper and lower envelopments experienced significant fluctuations at the starting and end points, which significantly distorted the decomposition result and led to an endpoint effect. Compared with the DWT, the SNR of VMD with $K = 5$ was observed to increase from 40.8201 to 42.6451, and the RMSE decreased from 2.2127 to 1.7934 (Table 2), suggesting that the data preprocessing method of VMD performed better than that of the DWT. In summary, the denoising performance of VMD was the best among those data preprocessing techniques.

As the chaotic noise in the observed ET time series was unknown, the PCC between the denoised ET time series and the residuals of each data preprocessing technique was computed to demonstrate the existence of chaotic noise in the collected ET time series; and the results were 0.1293, −0.04 and 0.0202, suggesting that our collected ET time series were disturbed by some types of noise. Eliminating chaotic noise from the observed datasets would be necessary for more credible estimation results.

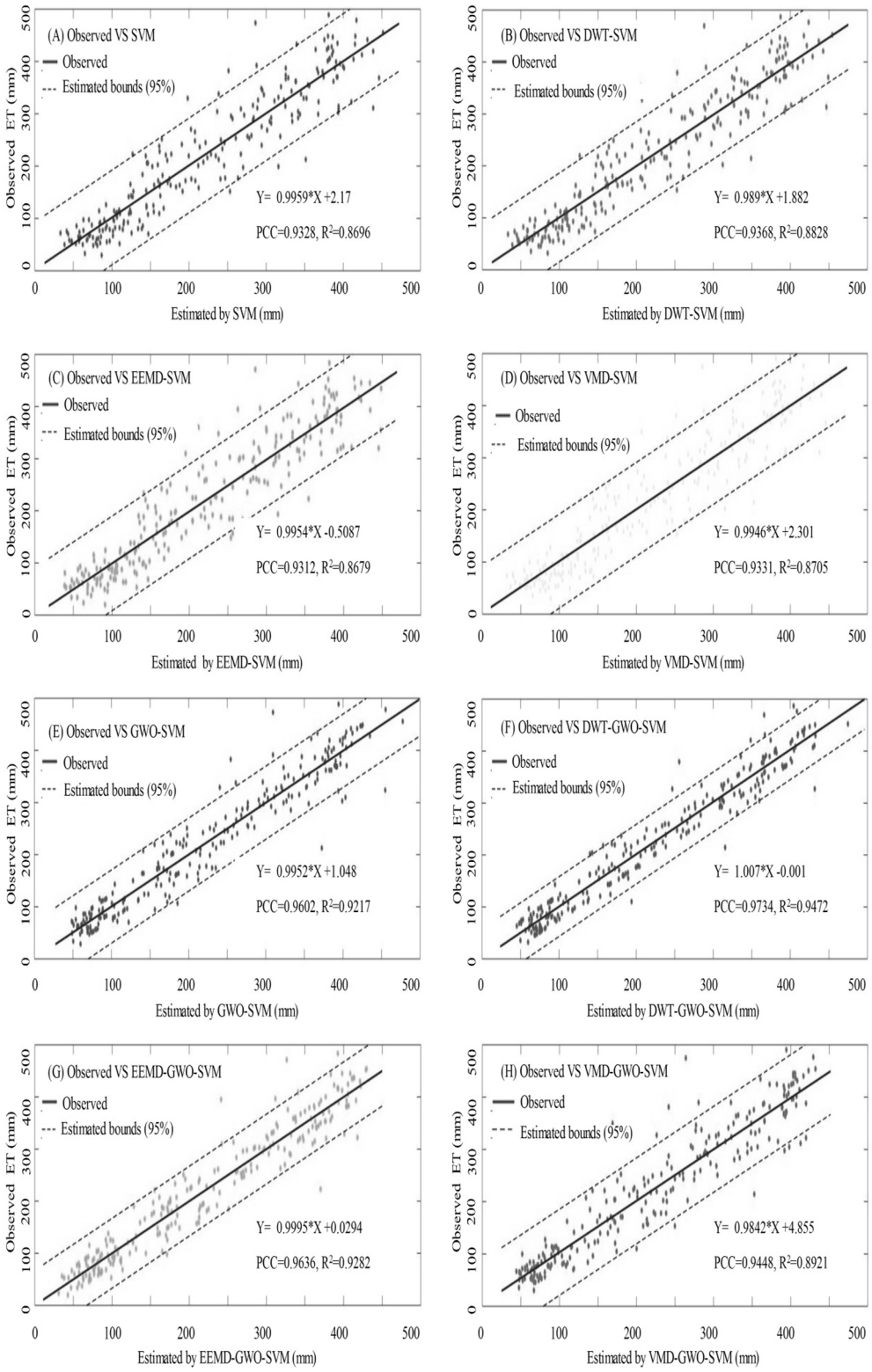

Fig. 6. The estimating performance of proposed models in the training stage.

3.2. Evaluation of the proposed models

The proposed models were used to estimate the monthly ET, and the parameter set for each model found during training that was then used for testing is shown in Table 3. The MAPE was chosen as the final benchmark among all the evaluation indicators to determine the optimal parameters of each proposed model. The optimal input dimensions of the SVM, DWT-SVM, EEMD-SVM, VMD-SVM, and VMD-GWO-SVM were 3; and the optimal input dimensions of the GWO-SVM, DWT-GWO-SVM and EEMD-GWO-SVM were 4, which were obtained by comparing the MAPE of each proposed model with different input dimensions (Table 3). The penalty coefficient and the radius of the kernel function of the SVM, DWT-SVM, EEMD-SVM and VMD-SVM were 1 and $1/d$, respectively. The purpose of choosing the hyperparameters of the SVM

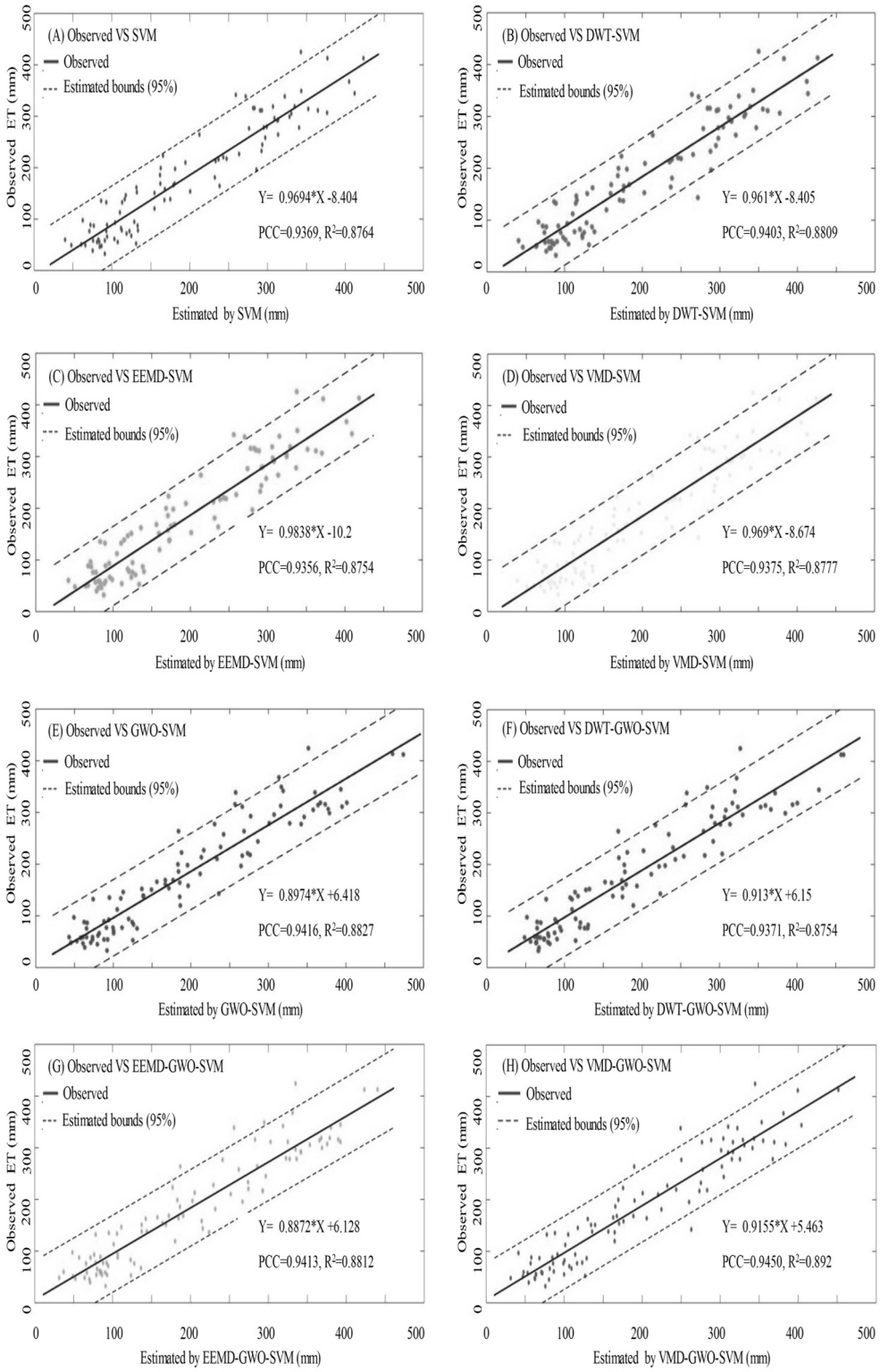

Fig. 7. The estimating performance of proposed models in the testing stage.

as the default values was to conveniently compare the effects of data preprocessing and parameter optimization on the estimation performance. As for the models integrated with the GWO algorithm, the number of search agents was 20, and the range of the penalty coefficient and the radius of the kernel function were [0.01, 100]. For each fixed input dimension d, including$d$ = 2, 3, 4, 5, and 6, the optimal hyperparameters of the SVM and the estimated results of the hybrid GWO-SVM, DWT-GWO-SVM, EEMD-GWO-SVM and VMD-GWO-SVM models were chosen according to the minimum MAPE from 5 replications.

Table 3 shows that the parameters used for model building influenced each other, and varying the value of one parameter inevitably resulted in a change in the other parameters. The estimation accuracy of the proposed models with different input dimensions had significant differences regardless of whether the hyperparameters of the SVM were fixed or optimized. For each fixed input dimension, the effects of data preprocessing and parameter optimization on the estimation accuracy

Table 4
The computing performance of proposed models in training and testing stages with the optimal parameters.

Estimating model	Training						Testing					
	NSCE	PCC	MAPE	NMSE	RMSE	MAE	NSCE	PCC	MAPE	NMSE	RMSE	MAE
SVM	0.8700	0.9328	18.89%	0.0909	45.5818	33.9835	0.8588	0.9369	28.42%	0.1740	40.3111	33.4904
DWT-SVM	0.8775	0.9368	18.23%	0.0850	44.2475	32.8495	0.8633	0.9403	27.94%	0.1665	39.6668	32.9807
EEMD-SVM	0.8671	0.9312	18.99%	0.0984	46.0874	34.7602	0.8596	0.9356	28.65%	0.1779	40.1962	33.3937
VMD-SVM	0.8705	0.9331	19.10%	0.0937	45.4876	34.0165	0.8591	0.9375	27.46%	0.1760	40.2667	33.4178
GWO-SVM	**0.9254**	**0.9621**	**15.47%**	**0.0474**	**34.542**	**25.3157**	**0.8575**	**0.9416**	**24.56%**	**0.1303**	**40.4901**	**32.7588**
DWT-GWO-SVM	**0.9479**	**0.9737**	**13.76%**	**0.0346**	**28.8268**	**22.3948**	**0.8593**	**0.9371**	**23.77%**	**0.1021**	**40.2469**	**32.6383**
EEMD-GWO-SVM	**0.9344**	**0.9667**	**15.77%**	**0.0533**	**32.2793**	**24.7613**	**0.8477**	**0.9413**	**26.67%**	**0.1472**	**41.866**	**34.7280**
VMD-GWO-SVM	**0.8923**	**0.9448**	**16.98%**	**0.0544**	**41.4806**	**29.7499**	**0.8754**	**0.9450**	**23.22%**	**0.1122**	**37.8756**	**30.2081**

Note: The performance indexes average of the models integrated with GWO are marked in bold.

were significant. As shown in Table 3, the MAPEs of the hybrid models simultaneously accounted for parameter optimization, and the data preprocessing decreased to varying degrees when compared with the single SVM model, implying that the estimation accuracy was significantly improved by combining the data preprocessing techniques and GWO algorithms with the SVM.

The results of the proposed models with the optimal parameters are shown in Fig. 5. Fig. 5 shows that all the proposed models could be employed to estimate the monthly ET with high computing accuracy by using only historical ET time series. The estimated values were on par with the observed middle range ET values, which constituted the majority of dataset points. The extremely high and low values were overestimated, especially in the testing stage.

In order to illustrate the practicability and effectiveness of the proposed models, scatter plots of the computing results and observed values in the training and testing stages are shown in Figs. 6 and 7, respectively. The estimation performance of any model was better in training than in testing, and the scatter diagrams of the observed and estimated monthly ET values in the training stage show that the slopes of the fitted lines were all less than 1 except for that of the hybrid DWT-GWO-SVM model (Fig. 6). Furthermore, the regression coefficients between the observed and estimated values were all less than 1 in the testing stage (Fig. 7), indicating that all the proposed models somewhat overestimated the monthly ET. Overall, the hybrid GWO-SVM, DWT-GWO-SVM, EEMD-GWO-SVM, and VMD-GWO-SVM models with the optimal hyperparameters showed better performance than the hybrid DWT-SVM, EEMD-SVM, VMD-SVM and SVM models with default hyperparameters (Figs. 6 and 7).

The computing accuracies of the proposed models were assessed both in the training and testing stages; and the results of evaluation indexes, including NSCE, PCC, MAPE, NMSE, RMSE and MAE, are illustrated in Table 4. The average performance indexes of the hybrid GWO-SVM, DWT-GWO-SVM, EEMD-GWO-SVM and VMD-GWO-SVM models with the optimal input dimensions were obtained via 5 replications because the outputs of the models integrated with GWO were random. The results of different evaluation indexes with the same evaluation direction were found to be inconsistent with each other on certain occasions. To avoid confusion in the evaluation processes caused by multiple evaluation indexes, the NSCE and MAPE were chosen as the main benchmarks.

Table 4 shows that the SVM has its own advantages in the monthly ET computing procedure. However, the computing accuracy of the SVM should be improved by choosing the best data preprocessing technique. As shown in Table 4, the computing performance of the hybrid DWT-SVM and VMD-SVM models was better than that of the SVM, suggesting that both the DWT and VMD effectively extracted the basic characteristics from nonstationary ET time series and improved the calculation accuracy. The estimation performance of the hybrid EEMD-SVM model was not found to be improved because the output of EEMD was distorted to some extent due to endpoint effects. This indicates that relying on one data preprocessing technique alone did not necessarily counterbalance the weakness of directly estimating ET, leading to large errors. Overall, the computing performance of the hybrid VMD-SVM model was better than those of the DWT-SVM, EEMD-SVM and SVM because the MAPE was observed to decrease from 28.42% to 27.46% in the testing stage.

Table 4 shows that the hybrid GWO-SVM model exhibited higher estimation accuracy than the hybrid DWT-SVM, EEMD-SVM, and VMD-SVM and single SVM models. The MAPE decreased from 28.42% to 24.56%, suggesting that the SVM hybridized with the GWO algorithm effectively improved the estimation performance. The optimization of parameters was crucially important to obtain more precise estimation results.

Compared with the hybrid GWO-SVM model, the estimation performance of the hybrid EEMD-GWO-SVM model was not better than that of the hybrid GWO-SVM model due to the endpoint effects of EEMD. Although there is a systematic overestimation in each proposed estimation model, the estimation performance of the DWT-GWO-SVM and VMD-GWO-SVM were better than that of the GWO-SVM. The positive indicators increased and the negative indicators decreased to varying degrees. Compared with the hybrid DWT-GWO-SVM model, the hybrid VMD-GWO-SVM model exhibited higher computing accuracy than the hybrid DWT-GWO-SVM model. The NSCE increased from 0.8593 to 0.8754 and the MAPE decreased from 23.77% to 23.22% in the testing stage, suggesting that choosing the best data preprocessing technique and optimal parameters by trial and error were crucially important to obtain the optimal estimation results. The best estimation model was obtained only by fully considering the factors that affected the accuracy of the estimation results.

Overall, the positive and negative indicators in Table 4 showed that the computing performance of the hybrid VMD-GWO-SVM model was the best among the proposed models. The NSCE was observed to increase from 0.8588 to 0.8754 and the MAPE was found to decrease from 28.42% to 23.22% in the testing stage. Thus, we suggest that the hybrid VMD-GWO-SVM model will be the best choice for estimating ET in the absence of regional meteorological monitoring.

4. Conclusions

This paper presents an application of the SVM hybridized with the GWO algorithm and data preprocessing methods, including the DWT, EEMD and VMD, for accurately estimating the monthly ET using only historical ET time series. Different from the existing ET estimation models, the proposed estimation model simultaneously conducts parameter optimization and the selection of data preprocessing techniques and requires fewer meteorological parameters for observation. Numerical simulation results showed that the hybrid VMD-GWO-SVM model exhibited superior computational performance over other

methods, and thus the method could be highly recommended for estimating ET without adequate meteorological parameters.

Declaration of Competing Interest

The authors declare that they have no known competing financial interests or personal relationships that could have appeared to influence the work reported in this paper.

Acknowledgements

The research was jointly supported by the National Key Research and Development Program of China (2018YFC0406603) and the National Natural Science Foundation of China (Nos. 41621001, 32061123006).

Appendix A. Supplementary data

The principle of mathematical methods used in this paper are illustrated in the Appendix.

Supplementary data to this article can be found online at https://doi.org/10.1016/j.jhydrol.2021.126881.

References

Abdullah, S.S., Malek, M.A., Abdullah, N.S., Kisi, O., Yap, K.S., 2015. Extreme Learning Machines: A new approach for prediction of reference evapotranspiration. J. Hydol. 527, 184–195.

Allen, R.G., Pruitt, W.O., 1991. FAO-24 reference evapotranspiration factors. J. Irrig. Drain. Eng. ASCE. 117 (5), 758–773.

Dong, Y., Wang, J., Xiao, L., Fu, T., 2021. Short-term wind speed time series forecasting based on a hybrid method with multiple objective optimization for non-convex target. Energy 215, 119180. https://doi.org/10.1016/j.energy.2020.119180.

Dragomiretskiy, K., Zosso, D., 2014. Variational Mode Decomposition. IEEE Trans. Signal Proces. 62 (3), 531–544.

Eagleson, P.S., 2002. Ecohydrology: Darwinian Expression of Vegetation Form and Function. Cambridge University Press.

Fan, J., Yue, W., Wu, L., Zhang, F., Cai, H., Wang, X., Lu, X., Xiang, Y., 2018. Evaluation of SVM, ELM and four tree-based ensemble models for predicting daily reference evapotranspiration using limited meteorological data in different climates of China. Agr. Forest Metoorol. 263, 225–241.

Feng, Y.u., Cui, N., Zhao, L.u., Hu, X., Gong, D., 2016. Comparison of ELM, GANN, WNN and empirical models for estimating reference evapotranspiration in humid region of Southwest China. J. Hydrol. 536, 376–383.

Feng, Y.u., Cui, N., Gong, D., Zhang, Q., Zhao, L.u., 2017. Evaluation of random forests and generalized regression neural networks for daily reference evapotranspiration modelling. Agric. Water Manage. 193, 163–173.

Fu, T., Zhang, S., Wang, C., 2020. Application and research for electricity price forecasting system based on multi-objective optimization and sub-models selection strategy. Soft Comput. 24 (20), 15611–15637.

Gocić, M., Motamedi, S., Shamshirband, S., Petković, D., Ch, S., Hashim, R., Arif, M., 2015. Soft computing approaches for forecasting reference evapotranspiration. Comput. Electron. Agric. 113, 164–173.

Gocic, M., Petković, D., Shamshirband, S., Kamsin, A., 2016. Comparative analysis of reference evapotranspiration equations modelling by extreme learning machine. Comput. Electron. Agric. 127, 56–63.

Hargreaves, G.H., Samani, Z.A., 1985. Reference crop evapotranspiration from temperature. Trans. ASAE 1 (2), 96–99.

Jain, S.K., Nayak, P.C., Sudheer, K.P., 2008. Models for estimating evapotranspiration using artificial neural networks, and their physical interpretation. Hydrol. Process. 22 (13), 2225–2234.

Keskin, M.E., Terzi, Ö., 2006. Artificial neural network models of daily pan evaporation. J. Hydro. Eng. 11 (1), 65–70.

Li, X.R., Zhang, Z.S., Liu, Y.B., Li., Yang, H.T., 2016. Fundamental Ecohydrology of Ecological Restoration and Recovery in Sand Desert Regions of China. Science Press.

Li, X.R., Jia, R.L., Zhang, Z.S., Zhang, P., Hui, R., 2018. Hydrological response of biological soil crusts to global warming: A ten year simulative study. Glob Change Biol. 24(10):4960-4971.

Liu, C., Cui, N., Gong, D., Hu, X., Feng, Yu, 2020. Evaluation of seasonal evapotranspiration of winter wheat in humid region of East China using large-weighted lysimeter and three models. J. Hydrol. 590, 125388. https://doi.org/10.1016/j.jhydrol.2020.125388.

Zhu, B., Feng, Y., Gong, D., Jiang, S., Zhao, L., Cui, N., 2020. Hybrid particle swarm optimization with extreme learning machine for daily reference evapotranspiration prediction from limited climatic data. Comput. Electron. Agric. 173, 105430. https://doi.org/10.1016/j.compag.2020.105430.

Malik, A., Kumar, A., Kisi, O., 2018. Daily pan evaporation estimation using heuristic methods with gamma test. J. Irrig. Drain. Eng. 144 (9), 04018023. https://doi.org/10.1061/(ASCE)IR.1943-4774.0001336.

Majhi, B., Naidu, D., Mishra, A.P., Satapathy, S.C., 2019. Improved prediction of daily pan evaporation using Deep-LSTM model. Neural Comput. Appl. 32 (12), 7823–7838.

Mehdizadeh, S., Behmanesh, J., Khalili, K., 2017. Using MARS, SVM, GEP and empirical equations for estimation of monthly mean reference evapotranspiration. Comput. Electron. Agric. 139, 103–114.

Mirjalili, S., Mirjalili, S.M., Lewis, A., 2014. Grey Wolf Optimizer. Adv. Eng. Softw. 69, 46–61.

Moazenzadeh, R., Mohammadi, B., Shamshirband, S., Chau, K.W., 2018. Coupling a firefly algorithm with support vector regression to predict evaporation in northern Iran. Eng. Appl. Comput. Fluid Mech. 12 (1), 584–597.

Pammar, L., Deka, P.C., 2017. Daily pan evaporation modeling in climatically contrasting zones with hybridization of wavelet transform and support vector machines. Paddy Water Environ. 15 (4), 711–722.

Petković, D., Gocic, M., Shamshirband, S., Qasem, S.N., Trajkovic, S., 2016. Particle swarm optimization-based radial basis function network for estimation of reference evapotranspiration. Theor. Appl. Climatol. 125 (3-4), 555–563.

Priestley, C., Taylor, R.J., 1972. On the assessment of surface heat flux and evaporation using large-scale parameters. Monthly Weather Rev. 100 (2), 81–92.

Rezaie-balf, M., Naganna, S.R., Ghaemi, A., Deka, P.C., 2017. Wavelet coupled MARS and M5 Model Tree approaches for groundwater level forecasting. J. Hydrol. 553, 356–373.

Rezaie-Balf, M., Kisi, O., Chua, L.H., 2019. Application of ensemble empirical mode de composition based on machine learning methodologies in forecasting monthly pan evaporation. Hydrol. Res. 50 (2), 498–516.

Rodríguez-Iturbe, I., Porporato, A., 2004. Ecohydrology of water-controlled ecosystems. Cambridge University Press, Soil moisture and plant dynamics.

Shiri, J., Kişi, Ö., Landeras, G., López, J.J., Nazemi, A.H., Stuyt, L.C.P.M., 2012. Daily reference evapotranspiration modeling by using genetic programming approach in the Basque Country (Northern Spain). J. Hydrol. 414-415, 302–316.

Traore, S., Luo, Y., Fipps, G., 2016. Deployment of artificial neural network for short-term forecasting of evapotranspiration using public weather forecast restricted messages. Agric. Water Manage. 163, 363–379.

Vapnik, V., 1998. Statistical learning theory. Wiley, NY.

Wang, L., Niu, Z., Kisi, O., Li, C., Yu, D., 2017. Pan evaporation modeling using four different heuristic approaches. Comput. Electron. Agric. 140, 203–213.

Wang, J., Wang, S., Yang, W., 2019. A novel non-linear combination system for short-term wind speed forecast. Renew. Energ. 143, 1172–1192.

Wen, X., Si, J., He, Z., Wu, J., Shao, H., Yu, H., 2015. Support-vector-machine-based models for modeling daily reference evapotranspiration with limited climatic data in extreme arid regions. Water Resour. Manage. 29 (9), 3195–3209.

Wu, L.F., Huang, G.M., Fan, J.L., Ma, X., Zhou, H.M., Zeng, W.Z., 2020. Hybrid extreme learning machine with meta-heuristic algorithms for monthly pan evaporation prediction. Comput Electron Agr. 168, 105–115.

Wu, Z., Huang, N.E., 2009. Ensemble empirical mode decomposition: a noise-assisted data analysis method. Adv. Adapt. Data Anal. 01 (01), 1–41.

Yin, Z., Wen, X., Feng, Q., He, Z., Zou, S., Yang, L., 2017. Integrating genetic algorithm and support vector machine for modeling daily reference evapotranspiration in a semi-arid mountain area. Hydrol. Res. 48,1177–1191.

Zhao, X., Wang, C., Su, J., Wang, J., 2019. Research and application based on the swarm intelligence algorithm and artificial intelligence for wind farm decision system. Renew. Energ. 134, 681–697.

Zuo, G., Luo, J., Wang, N., Lian, Y., He, X., 2020. Decomposition ensemble model based on variational mode decomposition and long short-term memory for streamflow forecasting. J. Hydrol. 585, 124776. https://doi.org/10.1016/j.jhydrol.2020.124776.